AMERICAN SOCIETY FOR MICROBIOLOGY | Infection and Immunity®

MOLECULAR PATHOGENESIS

# *Salmonella*-Mediated Inflammation Eliminates Competitors for Fructose-Asparagine in the Gut

**Jikang Wu,[a] Anice Sabag-Daigle,[b] Mikayla A. Borton,[c] Linnea F. M. Kop,[c] Blake E. Szkoda,[a,g] Brooke L. Deatherage Kaiser,[d] Stephen R. Lindemann,[e] Ryan S. Renslow,[e] Siwei Wei,[e] Carrie D. Nicora,[e] Karl K. Weitz,[e] Young-Mo Kim,[e] Joshua N. Adkins,[e] Thomas O. Metz,[e] Prosper Boyaka,[f] Venkat Gopalan,[a] Kelly C. Wrighton,[c] Vicki H. Wysocki,[a] Brian M. M. Ahmer[b]**

[a]Department of Chemistry and Biochemistry, The Ohio State University, Columbus, Ohio, USA
[b]Department of Microbial Infection and Immunity, The Ohio State University, Columbus, Ohio, USA
[c]Department of Microbiology, The Ohio State University, Columbus, Ohio, USA
[d]Signature Sciences and Technology Division, Pacific Northwest National Laboratory, Richland, Washington, USA
[e]Biological Sciences Division, Pacific Northwest National Laboratory, Richland, Washington, USA
[f]Department of Veterinary Biosciences, The Ohio State University, Columbus, Ohio, USA
[g]The Ohio State Biochemistry Program, The Ohio State University, Columbus, Ohio, USA

**ABSTRACT** *Salmonella enterica* elicits intestinal inflammation to gain access to nutrients. One of these nutrients is fructose-asparagine (F-Asn). The availability of F-Asn to *Salmonella* during infection is dependent upon *Salmonella* pathogenicity islands 1 and 2, which in turn are required to provoke inflammation. Here, we determined that F-Asn is present in mouse chow at approximately 400 pmol/mg (dry weight). F-Asn is also present in the intestinal tract of germfree mice at 2,700 pmol/mg (dry weight) and in the intestinal tract of conventional mice at 9 to 28 pmol/mg. These findings suggest that the mouse intestinal microbiota consumes F-Asn. We utilized heavy-labeled precursors of F-Asn to monitor its formation in the intestine, in the presence or absence of inflammation, and none was observed. Finally, we determined that some members of the class *Clostridia* encode F-Asn utilization pathways and that they are eliminated from highly inflamed *Salmonella*-infected mice. Collectively, our studies identify the source of F-Asn as the diet and that *Salmonella*-mediated inflammation is required to eliminate competitors and allow the pathogen nearly exclusive access to this nutrient.

**KEYWORDS** *Salmonella*, *Clostridium*, fructosamines, fructose-asparagine, Amadori products, Maillard reaction, inflammation, gut inflammation

*Salmonella* is among the most burdensome of foodborne pathogens in the United States and globally, causing 100 million illnesses and 50,000 deaths each year (1–7). *Salmonella* thrives in the host environment by inducing inflammation in order to disrupt the normal microbiota, allowing nutrients to accumulate and to generate electron acceptors for respiration (8–20). One of these nutrients is fructose-asparagine (F-Asn; Fig. 1) (21). F-Asn is an Amadori product generated from glucose and asparagine. Amadori products are formed by the nonenzymatic condensation of the carbonyl group of reducing sugars and the amino group of amino acids and proceed through the formation of a Schiff base that spontaneously rearranges to form a stable ketoamine (22–26). The Amadori product is the first stable compound in the sequence of reactions collectively referred to as the Maillard reaction (22, 27). The ability of *Salmonella* to utilize F-Asn is encoded by five horizontally acquired genes located between the conserved genes *gor* and *treF* (Fig. 1). Four of the genes appear to be in an operon, *fraBDAE*, while the fifth, *fraR*, is located upstream and is predicted to encode a transcription regulator of the GntR family. FraE is a periplasmic fructose-asparaginase

**Received** 3 January 2018 **Accepted** 20 February 2018

**Accepted manuscript posted online** 26 February 2018

**Citation** Wu J, Sabag-Daigle A, Borton MA, Kop LFM, Szkoda BE, Deatherage Kaiser BL, Lindemann SR, Renslow RS, Wei S, Nicora CD, Weitz KK, Kim Y-M, Adkins JN, Metz TO, Boyaka P, Gopalan V, Wrighton KC, Wysocki VH, Ahmer BMM. 2018. *Salmonella*-mediated inflammation eliminates competitors for fructose-asparagine in the gut. Infect Immun 86:e00945-17. https://doi.org/10.1128/IAI.00945-17.

**Editor** Vincent B. Young, University of Michigan—Ann Arbor



Address correspondence to Vicki H. Wysocki, wysocki.11@osu.edu, or Brian M. M. Ahmer, ahmer.1@osu.edu.

J.W. and A.S.-D. are co-first authors, and M.A.B., L.F.M.K., and B.E.S. are co-second authors.

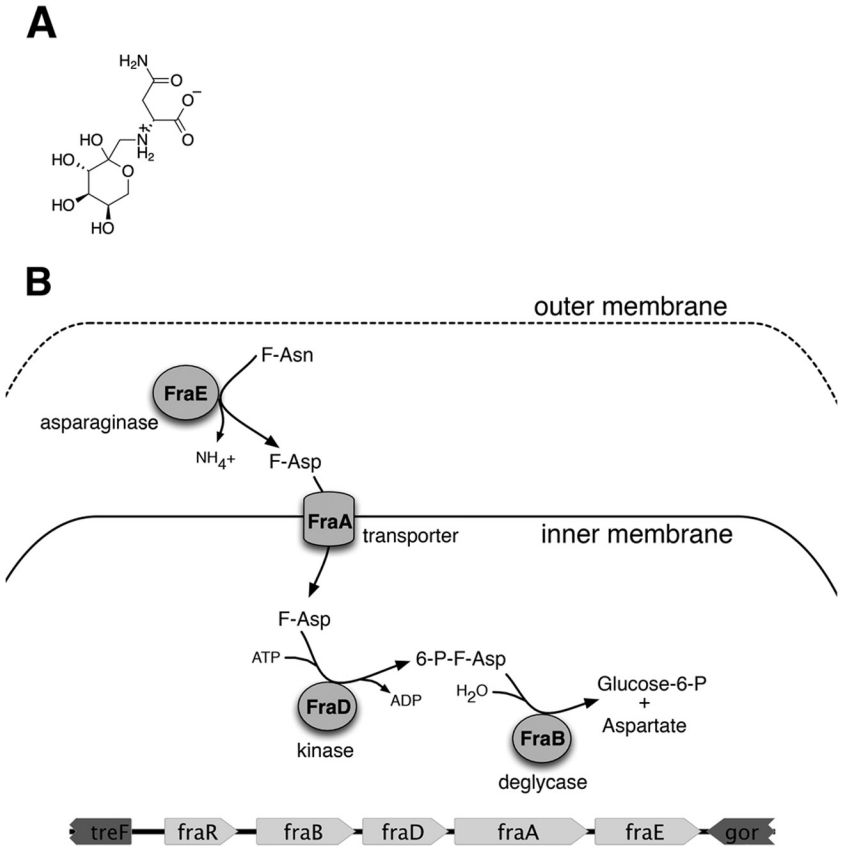


**FIG 1** Structure of F-Asn (A) and schematic of the F-Asn utilization pathway as well as the *fra* locus (B).

that releases ammonia from F-Asn to form fructose-aspartate (F-Asp) (28). F-Asp is likely transported to the cytoplasm by FraA, a Dcu-type transporter (anaerobic $C_4$-dicarboxylate), before its phosphorylation by the sugar kinase FraD. The resulting 6-phosphofuctose-aspartate (6-P-F-Asp) is then cleaved by the deglycase FraB, yielding glucose-6-phosphate (glucose-6-P) and aspartate (Fig. 1) (29, 30).

A genetic screen revealed that the *fra* locus is required for *Salmonella* fitness in a variety of mouse colitis models (21). Interestingly, this locus was not required for fitness in conventional mice, unless those mice had been pretreated with streptomycin to disrupt their intestinal microbiota. Conventional mice are highly resistant to the inflammation induced by *Salmonella*, but disruption of the microbiota using streptomycin increases susceptibility to *Salmonella*-mediated inflammation (31–34). Thus, the *fra* locus was required for fitness only in mice with an inflamed intestinal tract (21), a finding that was further supported by the observation that the *fra* locus was not required for fitness when the *fra* mutation was present in a *Salmonella* strain that could not induce inflammation (a mutant lacking *Salmonella* pathogenicity island 1 [SPI1] and SPI2 [the ΔSPI1 ΔSPI2 mutant]) (21). Follow-up studies determined that F-Asn is not an essential nutrient during infection of the inflamed gut (there are redundant nutrient sources) but, rather, that F-Asn is toxic to a *fraB* mutant of *Salmonella* (30). Mutants lacking other genes of the *fra* locus or even deletion of the entire *fra* locus had no detectable effect on *Salmonella* fitness in mice. FraB is the last enzyme in the F-Asn utilization pathway, and the absence of this enzyme leads to the accumulation of a toxic metabolite, 6-P-F-Asp. Deletion of the entire locus (*fraR fraBDAE*) does not lead to accumulation of 6-P-F-Asp, because the transporter and kinase are required for formation of 6-P-F-Asp (Fig. 1) (30).

Other *Salmonella* nutrient sources include 1,2-propanediol, which is derived from the microbiota (35); ethanolamine, which is derived from damaged cells (14); glucarate

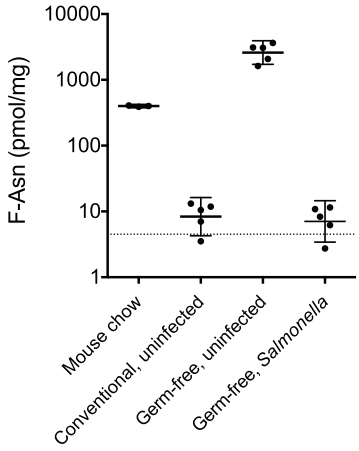


**FIG 2** Presence of F-Asn in mouse chow, conventional mouse cecum, germfree mouse cecum, and germfree mouse cecum infected with *Salmonella*. Each data point represents a mouse chow pellet (LabDiet recipe 5066) (3 data points) or a Swiss Webster mouse cecum at 1 day postinfection (5 data points each), with the geometric mean indicated by a horizontal line and error bars representing 95% confidence intervals. The limit of detection (4.5 pmol/mg) is indicated by the dotted line.

and galactarate, which are derived from *Nos2*-mediated oxidation of glucose and galactose (9); and L-lactate, which is derived from altered host metabolism (36). Here, we determined that F-Asn is derived from the diet (mouse chow) and that the fitness defect of the *fraB* mutant is related to the availability of F-Asn in the intestinal tract. When F-Asn is available, the *fraB* mutant is inhibited. We found that F-Asn is not depleted in germfree mice but is consumed by the microbiota in conventional mice. We previously identified several members of the *Clostridia* class that utilize F-Asn (37). Here, we found that these organisms are eliminated from the intestinal tract during *Salmonella*-mediated inflammation. Thus, inflammation is required for *Salmonella* to eliminate competing consumers and gain nearly exclusive access to this nutrient.

## RESULTS

**F-Asn is derived from the diet rather than the microbiota.** A *fraB* mutant of *Salmonella* is dramatically attenuated in germfree mice and in other mouse models that are susceptible to *Salmonella*-induced inflammation (21). The *fraB* mutant is attenuated due to the accumulation of a toxic metabolic intermediate, 6-P-F-Asp, during utilization of F-Asn as a carbon or nitrogen source (30). However, the *fraB* mutant is not attenuated in conventional mice. These results suggest that there is F-Asn within the intestinal tract of germfree mice but not in that of conventional mice, where other organisms presumably consume F-Asn and decrease F-Asn availability to *Salmonella*. To test this hypothesis, we used mass spectrometry (MS) to measure the F-Asn concentration in the cecal contents of germfree and conventional Swiss Webster mice (Fig. 2). F-Asn was detected in the intestines of germfree mice (2,700 pmol/mg), suggesting that mice cannot alter or metabolize the F-Asn that is within the gastrointestinal tract. This concentration is higher than what was observed in the mouse chow (400 pmol/mg), suggesting that either F-Asn may accumulate or F-Asn can form in the mouse gastrointestinal tract (see below). The concentration of F-Asn is much lower (8 pmol/mg) in the ceca of germfree mice infected with *Salmonella*, consistent with the ability of *Salmonella* to consume and utilize F-Asn. The concentration of F-Asn was also very low in the cecum of conventional mice (9 pmol/mg), consistent with the hypothesis that some member(s) of the normal microbiota can utilize F-Asn. These measurements were repeated with a slightly different MS protocol and different samples, and similar results were observed (see Fig. S1 in the supplemental material).

**F-Asn does not form in the mouse intestinal tract.** The F-Asn concentration in the ceca of germfree mice is higher than that in mouse chow (Fig. 2 and S1). We

hypothesized that either F-Asn originated in the mouse chow and accumulated in the cecum or was formed *de novo* in the mouse gastrointestinal tract. To test the latter hypothesis, we provided five germfree mice with drinking water containing labeled precursors of F-Asn ($^{15}$N-labeled asparagine and $^{13}$C-labeled glucose) and then used MS to measure the labeled F-Asn in the cecal contents. No labeled F-Asn was detected in any of the samples. We then hypothesized that *de novo* formation may be dependent upon *Salmonella*-mediated inflammation. To test this hypothesis, we used three groups of five mice each, all of which were provided with labeled $^{15}$N-labeled asparagine and $^{13}$C-labeled glucose in their drinking water, as described above, and infected each of the groups with a different *Salmonella* strain. The first group received strain ASD215 (14028 Δ*fra80* Δ*ansB80*::Kan). This strain was used to eliminate the possibility of *Salmonella* consuming any newly formed F-Asn, as it lacks the *fra* locus and also lacks *ansB*, a periplasmic asparaginase that can convert F-Asn to F-Asp (28). Another group was infected with strain ASD203 (14028 ΔSPI1 ΔSPI2 Δ*fra4* Δ*ansB80*::Kan). This strain is similar to ASD215, except that it lacks SPI1 and SPI2 and thus cannot initiate inflammation (38). A third group was infected with *Salmonella* strain HMB175 (14028 Δ*ansB80*::Kan), which can consume F-Asn and can initiate inflammation. No labeled F-Asn was detected in any of the samples, suggesting that F-Asn is not formed within the murine gastrointestinal tract, regardless of whether the gastrointestinal tract is inflamed or not by *Salmonella* (MS data from one mouse infected with ASD215 are shown in Fig. S2; data for the rest of the mice are not shown).

**Competitors for F-Asn are eliminated by high levels of inflammation.** The gastrointestinal tracts of many mouse strains fail to become inflamed upon infection with *Salmonella*. The resistance to *Salmonella*-mediated inflammation appears to be due to the normal microbiota, since germfree mice are susceptible to *Salmonella*-mediated inflammation. Disruption of the microbiota by treatment with streptomycin or other antibiotics (31–34) increases susceptibility to *Salmonella*-mediated inflammation. However, the use of antibiotic-treated or germfree mice is not ideal for studying *Salmonella*-mediated inflammation and its effects on the microbiota. Therefore, we sought an alternative.

The CBA/J strain of mouse is unusual in that it allows *Salmonella* to persistently colonize the intestinal tract for a long period of time, which leads to inflammation after 8 to 14 days of infection (13, 39). We have previously used this model to study the microbiome disturbances caused by *Salmonella* (40). Here, we leveraged these earlier collected samples to quantify the F-Asn concentration in the ceca after 16 days and tested the hypothesis that disruption of the microbial community (by either inflammation or antibiotic treatment) causes F-Asn to accumulate in the intestinal tract. Such an expectation is based on the idea that inflammation eliminates members of the microbiota that would otherwise consume F-Asn (Fig. 3). Previously, we reported a relationship between *Salmonella* relative abundance and inflammation levels and identified two distinct *Salmonella* responses (a high response, in which there is a >46% *Salmonella* relative abundance in the cecum, and a low response, in which there is a <7% *Salmonella* relative abundance in the cecum) in mice treated with the same *Salmonella* inoculum (40). Inflammation, measured using lipocalin-2 as a marker (9, 41–44), correlated with the *Salmonella* response; i.e., inflammation was high when the *Salmonella* response was high. The F-Asn concentration was relatively low in all samples compared to that in the germfree mice (Fig. 2), but it was the highest in the highly inflamed samples (2,700 pmol/mg F-Asn in germfree mice compared to 100 pmol/mg in the high-*Salmonella*-responder samples) (Fig. 3). The lipocalin-2 concentrations observed in streptomycin-treated mice were not different than those observed in untreated control mice, indicating that the mice did not become inflamed from this treatment or that they had recovered by day 15. In fact, recovery by day 4 has been noted previously (36). The lipocalin-2 concentrations observed in dextran sulfate sodium (DSS)-treated mice were statistically significantly higher than those observed in the controls, but the practical significance was low (1 ng/g versus 3 ng/g). Consistent with the lack of

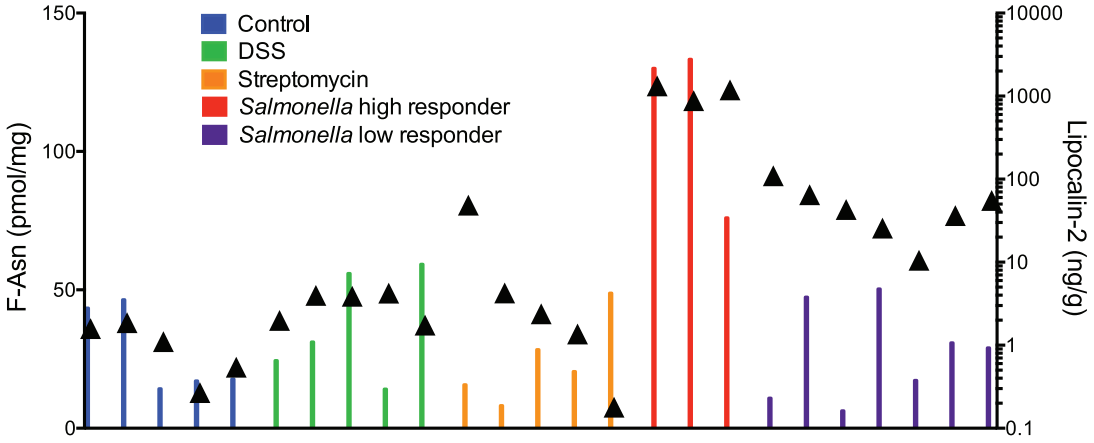


**FIG 3** F-Asn and lipocalin-2 concentrations in CBA/J mice. The F-Asn concentration in each individual mouse cecum at day 16 postinfection is indicated by a bar, with the color denoting the treatment. Mice infected with the same amount of *Salmonella* are denoted as high and low responders, with high responders having a >46% *Salmonella* relative abundance and low responders having a <7% *Salmonella* relative abundance (40). The lipocalin-2 concentration from feces collected on day 15 postinfection is indicated by a black triangle on each bar. The F-Asn concentrations in the high-*Salmonella*-responder group but no other groups were statistically significantly different than those in the control group (Mann-Whitney test, $P = 0.0357$). The lipocalin-2 concentrations in the DSS-treated, high-*Salmonella*-responder, and low-*Salmonella*-responder groups were all statistically significantly different than those in the control group (Mann-Whitney test, $P = 0.0159$, 0.0357, and 0.0025, respectively). The result for the high-*Salmonella*-responder group was statistically significantly different than that for all other groups (Mann-Whitney test, $P < 0.03$).

inflammation, the F-Asn concentrations in these groups were not statistically significantly different (28 pmol/mg in control mice, 24 pmol/mg in streptomycin-treated mice, and 37 pmol/mg in DSS-treated mice; Fig. 3).

Metagenomics analysis of one highly inflamed *Salmonella*-infected mouse (1,130 ng/g feces of lipocalin-2) and three uninfected control mice (76 ± 17 ng/g feces of lipocalin-2) showed that the number of distinct *fraBD* homologs was greatly decreased in the inflamed mouse. The three control fecal samples contained between 13 and 18 *fraB* and *fraD* homolog pairs, with each pair colocalized on the same contig. The majority of these contigs belonged to the *Firmicutes* (93% ± 1%), with the exception of an actinobacterial *Collinsella* contig that was detected in each of the control metagenomes. In the *Salmonella*-infected metagenome, only the *Salmonella fraBD* was detected, indicating that all other F-Asn consumers were eliminated from the *Salmonella*-infected gut. However, 70% of the reads in this sample were *Salmonella* reads. To account for differences in the underlying community richness or sequencing depth, the recovered *fraBD* homologs were normalized to the S3 ribosomal gene number. The relative abundance of non-*Salmonella fraBD*-containing organisms was 23% of the community in the noninflamed controls, whereas it was 0% in the *Salmonella*-infected sample (Fig. 4). This observation demonstrates that the ratio of putative F-Asn consumers to nonconsumers decreased in the *Salmonella*-infected sample compared to the noninflamed control sample.

Our metagenomics analyses revealed that *Salmonella* infection led to decreased *fraBD* gene diversity, presumably due to elimination of other F-Asn-consuming competitors. Because the cost-intensive metagenomics studies were performed with a single highly inflamed *Salmonella*-infected mouse and three control mice, we sought an alternative method where we could examine multiple samples in parallel for the presence or absence of a target sequence and thereby cross-validate the findings from sequencing of the mouse fecal DNA. Specifically, we examined if any member of the *Clostridia*, whose select representatives we recently validated catabolize F-Asn (37), decreased upon *Salmonella* infection. To fulfill this objective, we chose quantitative PCR (qPCR) as the method of choice.

We first identified a 21-nucleotide (nt) sequence present in the *fraB* gene of *Clostridium* sp. strain MGS:81 but not in *Salmonella fraB*. This sequence was used to

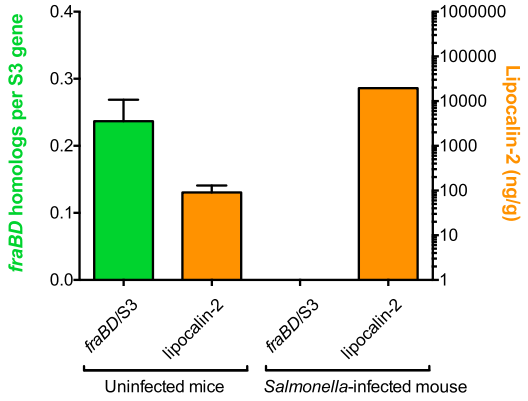


**FIG 4** *fraBD* homologs are eliminated during *Salmonella*-mediated inflammation. The ratio of *fraBD* homologs to S3 ribosomal protein genes detected in CBA/J mouse fecal metagenomes at day 11 postinfection is plotted on the left *y* axis (green). Measurements of the lipocalin-2 concentration in the feces of the same mice are plotted on the right *y* axis (orange).

design our qPCR probe. Moreover, we generated a 144-bp amplicon that encompasses the probe sequence and used it as our standard. We generated a standard curve using a 10-fold dilution series ranging from 10 pg to 1 fg of the clostridial *fraB* 144-bp amplicon (Fig. 5A and B). The threshold cycle ($C_T$) values ranged from 13 to 29 and led to a standard curve with a slope of −3.93 (~80% efficiency) and an $R^2$ value of 0.999. This standard curve was then used to determine the copy numbers in the genomic DNA (gDNA) samples from different mice.

We used qPCR assays to determine the *Clostridium* sp. MGS:81 copy number in five control, five DSS-treated, five streptomycin-treated, seven low-*Salmonella*-responder, and three high-*Salmonella*-responder mice (Fig. 5C). The copy numbers were calculated for all mice using the triplicate-averaged $C_T$ value from each and a nine-way averaged standard curve (Fig. 5B). After removal of outliers using Grubbs' tests (one DSS-treated mouse and one low-*Salmonella*-responder mouse), the average number of *Clostridium* sp. MGS:81 copies was calculated for each mouse type (Fig. 5D). Two-sample *t* tests (assuming unequal variances, with $\alpha = 0.05$) showed that the control, streptomycin-treated, DSS-treated, and low-*Salmonella*-responder mice each contained *Clostridium* sp. MGS:81 copy numbers statistically significantly different than those in the high-*Salmonella*-responder mice, but all other relationships between groups were not statistically significant. There was a striking decrease, if not complete elimination, of the clostridial representative in the high *Salmonella*-responder mice (Fig. 5D).

## DISCUSSION

*Salmonella* is one of the most significant foodborne pathogens affecting humans and livestock (1–7). Previously, we utilized a genetic screen to identify *Salmonella* genes required for optimal fitness in the gastrointestinal tract of germfree mice (21). The *fra* locus was identified in this screen and then further demonstrated to be extremely important for *Salmonella* fitness in several other mouse models (21). The fitness defect is observed only with *fraB* mutants and not with mutants lacking other genes of the *fra* locus (30). The fitness defect is not caused by a lack of F-Asn acquisition but, rather, is caused by the accumulation of a toxic metabolic intermediate, 6-P-F-Asp (30). The *fraB* fitness defect was observed only in mouse models that are susceptible to inflammation and was abrogated by additional mutations in the genes required for *Salmonella* to cause inflammation, the genes encoding SPI1 and SPI2 (21). Thus, the *Salmonella fraB* mutant has a fitness disadvantage only during gastrointestinal inflammation, which, we propose here, is simply due to the availability of F-Asn. Most mouse strains are resistant to *Salmonella*-mediated inflammation and become susceptible only after a perturbation of the microbiota, most commonly achieved with streptomycin (33, 34, 45, 46). Germfree mice are also susceptible (34). In this study, we measured the F-Asn concen-

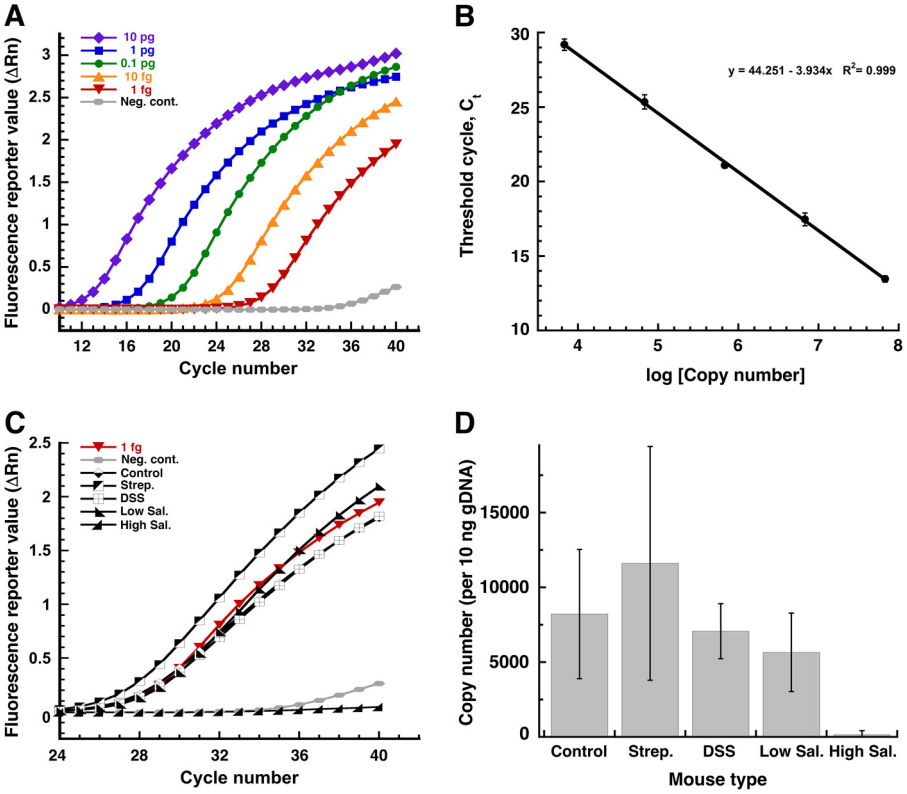


**FIG 5** qPCR analysis of gDNA samples isolated from the cecum of control, streptomycin-treated, DSS-treated, and low- and high-*Salmonella*-responder CBA/J mice at day 16 postinfection. (A) Amplification plots that indicate the change in normalized fluorescence (ΔRn) for the five indicated amounts of the 144-bp standard. (B) Standard curve of the threshold cycle ($C_T$) versus the copy number obtained using nine technical replicates for each standard. Error bars represent standard deviations of the mean values calculated using the data from nine replicates. (C) Amplification plots that indicate the ΔRn for the indicated mouse gDNA samples together with those obtained for the 1-fg standard and negative control. (D) *Clostridium* sp. MGS:81 copy number calculated using the $C_T$ values determined in the assay whose results are shown in panel C. Error bars represent standard deviations of the respective mean values calculated from triplicate measurements for each mouse. Neg. cont., negative control; Strep., streptomycin; Sal., *Salmonella*.

tration in a variety of mice and found that the concentrations are consistent with *fraB* phenotypes (a *fraB* mutant has a fitness defect only when F-Asn is present). In germfree Swiss Webster mice, F-Asn is abundant (2,700 ± 826 pmol/mg) (Fig. 2; see also Fig. S1 in the supplemental material), and a *Salmonella fraB* mutant is defective compared to the wild type in these mice (21). In conventional Swiss Webster mice, F-Asn is not abundant (9 ± 4 pmol/mg) (Fig. 2 and S1) and the *fraB* mutant is not defective compared to the wild type (21, 30).

The concentration of F-Asn is high in germfree mice and low in conventional mice, presumably because members of the microbiota consume F-Asn. We have determined that some members of the *Clostridia* class carry F-Asn utilization gene homologs (*fraB*, *fraD*, and *fraE*) and can consume F-Asn (37). If these members of the microbiota are drastically reduced in number during inflammation, then F-Asn would become available, and this availability would explain how the *Salmonella fraB* mutant becomes inhibited during inflammation. CBA/J is an unusual strain of mouse that can become inflamed by *Salmonella* without the need for a germfree state or antibiotic perturbation of the normal microbiota (13, 39). The CBA/J mouse allows a persistent colonization of the gastrointestinal tract that eventually leads to inflammation after 8 to 10 days. This is slow compared with the time to inflammation in antibiotic-treated mice (1 day), but the absence of antibiotics allows a more relevant study of the effects of *Salmonella* on the gut microbiota (13, 39, 40).

Using this CBA/J model, we determined that the inflammation achieved by *Salmonella* is quite variable but that the F-Asn concentration was the highest in the most highly inflamed mice (Fig. 3). The F-Asn concentration in these highly inflamed CBA/J mice was 113 ± 32 pmol/mg, which is much lower than the 2,700 pmol/mg present in germfree mice (presumably due to *Salmonella* consuming the F-Asn as it becomes available) but is higher than what is available in the uninfected conventional Swiss Webster (9 ± 4 pmol/mg) or CBA/J (28 ± 16 pmol/mg) mice. Since a *fraB* mutant is not inhibited in conventional mice but is inhibited in highly inflamed mice, the concentration of F-Asn required to inhibit the *fraB* mutant *in vivo* is therefore likely to be between 28 and 113 pmol/mg (or 28 and 113 $\mu$M, respectively). The 50% and 90% inhibitory concentrations ($IC_{50}$ and $IC_{90}$) of F-Asn for a *Salmonella fraB* mutant grown *in vitro* are 19 $\mu$M and 174 $\mu$M, respectively (30). Therefore, even with wild-type *Salmonella* consuming F-Asn, the F-Asn concentration (113 ± 32 pmol/mg [dry weight]) in the ceca of these highly inflamed CBA/J mice appears to be in a range that would be expected to inhibit a *Salmonella fraB* mutant.

While *Salmonella*-mediated inflammation led to increased F-Asn concentrations in CBA/J mice, we were curious if streptomycin or DSS treatment would give the same result. Streptomycin might negatively impact normal microbiota populations that consume F-Asn, leading to increasing concentrations of F-Asn. Similarly, DSS might inflame the gastrointestinal tract and decrease the populations of normal microbiota that consume F-Asn. However, streptomycin treatment did not cause lipocalin-2 or F-Asn concentrations to rise compared to those in untreated mice, suggesting that the F-Asn consumers are not susceptible to streptomycin, that the streptomycin did not kill a sufficient proportion of the consumers, or that the consumers had simply repopulated the intestine by the time that we took the samples (Fig. 3). Since the streptomycin treatment was a one-time administration and our measurements were 15 or 16 days later, repopulation is the most likely explanation (36). DSS treatment also failed to increase the lipocalin-2 or F-Asn concentrations. DSS was administered throughout the experiment, and the dose was high, so it is not clear why the CBA/J mice failed to become more inflamed. It has previously been noted that CBA mice predominantly become inflamed in the distal colon rather than the proximal colon, although the cecum was not tested (47). Also, while CBA mice were not tested, it has been determined that there is a wide range of responsiveness of mice to DSS (48).

Metagenomic analysis of the microbial community revealed that *Clostridia* carrying F-Asn utilization genes were abundant in the three uninfected control mice but absent from a highly inflamed *Salmonella*-infected mouse (Fig. 4). The metagenomic data from a single highly inflamed mouse showed that all species that carry *fraBD* homologs are eliminated. This change in the microbial landscape was confirmed for a single species of *Clostridium* using qPCR with all 25 of the mice, including the three highly inflamed *Salmonella*-infected mice (Fig. 3). This particular *Clostridium* species was essentially eliminated from all of the mice with a high *Salmonella* abundance, while its abundance in mice with a low *Salmonella* abundance or in the streptomycin- or DSS-treated mice was not different from that in the control mice (Fig. 5). This elimination of competitors would be expected to make F-Asn available to *Salmonella*. The availability of F-Asn can be determined most readily using a *fraB* mutant of *Salmonella* that is strongly inhibited by F-Asn. In all mouse models of inflammation that we have examined, the *fraB* mutant is inhibited, while in mice that are not inflamed, the *fraB* mutant is not inhibited (21, 30). Furthermore, the inhibition of the *fraB* mutant is absent when using a *Salmonella* genetic background lacking SPI1 and SPI2, which are required for *Salmonella*-mediated inflammation. These phenotypes of the *Salmonella fraB* mutant combined with the direct measurements of F-Asn performed here, both in mouse chow and in mouse intestines, provide strong evidence that the source of F-Asn is the diet (mouse chow) and that it becomes available to *Salmonella* upon inflammation-mediated elimination of competitors within the microbiota, predominantly of the *Clostridia* class.

In the original genetic screen in which we identified the *fra* locus, the *fraB* mutant was more attenuated in germfree mice monocolonized with *Enterobacter cloacae* than

it was in completely germfree mice (21). Since *Enterobacter cloacae* does not utilize F-Asn, we hypothesize that *E. cloacae* removed many of the nutrient sources that could be utilized by *Salmonella*, leaving a relatively high proportion of F-Asn. This same phenomenon is seen using *in vitro* toxicity assays in which medium containing F-Asn but depleted of other nutrients by the growth of other organisms is more toxic to the *Salmonella fraB* mutant than medium that has not been previously depleted by other organisms (37).

We have recently confirmed that *Clostridium acetobutylicum*, *C. bolteae*, and *C. clostridioforme* can utilize F-Asn during growth *in vitro* (37). We also identified numerous human foods that contain F-Asn (49). There are some foods that have as much F-Asn as mouse chow (400 pmol/mg or higher), including fresh apricots, lettuce, asparagus, and canned peaches, but far higher concentrations (11,000 to 35,000 pmol/mg) are found in heat-dried apricots, heat-dried apples, and heat-dried asparagus (49). Since the *fra* locus is far older than the human invention of heat drying of foods, the moderate concentrations of F-Asn present in fresh apricots, asparagus, etc. (at levels mirroring those in mouse chow), are likely responsible for *Salmonella*'s maintenance of the *fra* locus. It is not known if the presumably modern inventions of heat-dried fruits and vegetables can alter a *Salmonella* infection. Regular consumption of dried apricots may create a microbial community that is excellent at consuming F-Asn and actually increase resistance to *Salmonella*. On the other hand, a single meal of dried apricots by a person that does not normally consume them may temporarily increase susceptibility to *Salmonella*. These hypotheses remain to be tested.

## MATERIALS AND METHODS

**Bacterial strains and growth.** *Salmonella enterica* serovar Typhimurium strains were used throughout. The wild-type strain in Fig. S1 in the supplemental material is strain MA43 (IR715 *phoN*::*aadA*), and the *fraB* mutant is strain MA59 (IR715 *fraB1*::Kan) (21). IR715 is an ATCC 14028 derivative resistant to nalidixic acid (50). In all other figures, the wild type is strain ATCC 14028. HMB175 is ATCC 14028 Δ*ansB80*::Kan (28). ASD215 is ATCC 14028 Δ*fra80* Δ*ansB80*::Kan. It was constructed by using phage P22HTint to transduce the Δ*ansB80*::Kan allele from HMB107 (28) into HMB215 (30). ASD203 is ATCC 14028 Δ(*avrA-invH*)*1* Δ(*ssrB-ssaU*)*1* Δ(*fraR-fraBDAE*)*4* Δ*ansB80*::Kan. It was constructed by using phage P22HTint to transduce the Δ*ansB80*::Kan allele from HMB107 (28) into ASD202. ASD202 was constructed by using the FLP recombinase encoded on pCP20 to remove the kanamycin resistance cassette (Kan) from the *fra* island of strain ASD201 (38). All strains were grown overnight with shaking at 37°C in LB broth (Fisher Bioreagents).

**Animal experiments.** All animal work was performed using protocols approved by The Ohio State University Institutional Animal Care and Use Committee (IACUC; OSU 2009A0035). Conventional Swiss Webster mice were obtained from Taconic. The germfree mice were Swiss Webster mice obtained from the breeding colony at The Ohio State University. They were of mixed sex and of variable age (range, 6 weeks to 6 months old). They were fed irradiated chow recipe 5066 (LabDiet). Germfree mice were inoculated with *Salmonella* overnight cultures that had been centrifuged at 10,000 × *g* and resuspended in water. The bacterial suspension was diluted to $10^5$ CFU/ml in water and administered to mice by oral gavage with 100 μl ($10^4$ CFU total). At 1 day postinfection, the mice were euthanized for organ harvest.

The CBA/J mouse samples used in the assays whose results are shown in Fig. 3 and 5 were taken from a study published elsewhere (40). The lipocalin-2 results from these mice were published previously (40), but the F-Asn and qPCR data are unique to this report. New CBA/J mice were obtained for the metagenomic studies. All CBA/J mice were obtained from The Jackson Laboratory (Bar Harbor, ME), were females from 6 to 10 weeks old, and were fed chow recipe 7912 (Teklad). They were inoculated orally with *Salmonella* as described above for the germfree mice, except that they each received $10^9$ CFU total. Metagenomic libraries were prepared from day 11 fecal samples (see below), and the lipocalin-2 concentration was measured in fecal pellets from day 15 postinfection (40). At 16 days postinfection, the mice were euthanized for organ harvest and the F-Asn concentration in the cecal contents was determined as described below.

**Synthesis of fructose-asparagine and heavy fructose-asparagine.** Fructose-asparagine was synthesized as described previously (23). $^{13}$C-labeled fructose-asparagine was made with the same protocol but using glucose uniformly labeled with $^{13}$C (Cambridge Isotope Laboratories).

**LC-MS.** To measure the F-Asn concentrations from mouse ceca, the ceca were cut open and the contents were gently scraped from the inner surface and rinsed with water. The cecal contents were then stored at −80°C until further use. Prior to analysis, the cecal contents were lyophilized, weighed, and ground on dry ice with a pestle that fit 1.5-ml microcentrifuge tubes. Mouse chow (recipe 5066; LabDiet) samples were also lyophilized and ground on dry ice with a pestle in a 1.5-ml tube. For all sample types, approximately 10 mg of dry material was then transferred to a new preweighed 1.5-ml tube and weighed, followed by the addition of 500 μl chilled methanol and 500 μl $H_2O$ spiked with 0.16 nmol [$^{13}$C]F-Asn. After being vortexed and centrifuged at 14,800 × *g* for 1 h, the supernatant was transferred

into a new 1.5-ml centrifuge tube, frozen, and lyophilized. Before MS analysis, these dried pellets were resuspended in 500 $\mu$l acetonitrile-water (80%:20%) with 0.1% (vol/vol) formic acid (liquid chromatography [LC]-MS grade; Thermo Scientific) and filtered through a 0.2-$\mu$m-pore-size polytetrafluoroethylene filter (Thermo Scientific). The flowthrough was analyzed by LC coupled to MS. A nano-Acquity ultraperformance LC (UPLC) system (Waters, Milford, MA, USA) with a UPLC M-class BEH 130 amide column (75 $\mu$m by 100 mm; particle size, 1.7 $\mu$m; Waters) was coupled to a triple-quadrupole mass spectrometer (Xevo TQ-S; Waters) for F-Asn quantification. Buffer A (0.1% formic acid [FA] in water with 10% acetonitrile) and buffer B (0.1% FA in acetonitrile) were used as mobile phases for gradient separation, which started with 80% buffer B for 6 min at a flow rate of 0.5 $\mu$l/min and was then followed by the following gradient: from 6 to 20 min, 80 to 50% buffer B; from 20 to 26 min, 50% buffer B; from 26 to 28 min, 50 to 80% buffer B; from 28 to 35 min, 80% buffer B. The mass spectrometer was operated in positive-ion nanoelectrospray ionization mode (nano-ESI$^+$) with a capillary voltage of 3.5 kV, a source temperature of 70°C, a cone voltage of 2 V, and a source offset of 2 V. The gas flow rate for the collision cell was 0.15 ml/min. While transition *m/z* 295 → 211 of F-Asn with a collision energy of 13 eV was selected for quantitation, *m/z* 301 → 216 of [$^{13}$C]F-Asn with a collision energy of 13 eV was used for normalization. While *m/z* 295 → 211 was used as the quantifier, transitions *m/z* 295 → 277 and *m/z* 295 → 259 were used as qualifiers to verify the presence of F-Asn. Skyline-daily (v3.5; M. J. MacCoss lab, Department of Genome Sciences, University of Washington, Seattle, WA, USA) was used for calculating the peak area of transitions.

A Q Exactive mass spectrometer (Thermo Fisher Scientific) with a Nanospray Flex ion source coupled with the same LC system described above was used for detecting the *de novo* formation of F-Asn. The LC settings were the same as those described above, and the mass spectrometer was operated in positive mode with a capillary voltage at 1.68 kV, a source temperature at 350°C, and the S-lens level at 50. A full mass scan (*m/z* 50 to 750) was performed at a resolution of 35,000 with an automatic gain control (AGC) target at 3e$^6$ and a maximum injection time (IT) at 200 ms. Thirteen ions with *m/z* from 295.1 to 307.1, which differed by 1 Da in between, were selected for parallel reaction monitoring (PRM) scan with a resolution at 17,500, an automatic gain control (AGC) target at 1e$^6$, a maximum injection time (IT) at 100 ms, an isolation window at 0.7 *m/z*, and a stepped collision energy of 20 eV.

**Metagenomic profiling of FraBD from CBA/J mice.** Total nucleic acids were extracted from mouse fecal samples (day 11 postinfection) using a PowerSoil DNA isolation kit (MoBio), eluted in 100 $\mu$l of the elution buffer provided, and stored at −20°C until sequencing. DNA was submitted for sequencing to the Genomics Shared Resource facility at The Ohio State University. Libraries were prepared with the Nextera XT library system in accordance with methods described previously (51, 52). All analysis methods and accompanying scripts from assembly to gene annotation are provided in Github (https://github.com/TheWrightonLab). Known FraB and FraD amino acid sequences for *Salmonella enterica* LT2 were used to recover homologs (E value $< 1e^{-20}$) from each metagenome using the NCBI BLASTP program (53). The ratio of the recovered FraBD homologs to single-copy S3 ribosomal proteins (housekeeping gene) was used to estimate the relative abundance of F-Asn consumers in each sampled microbial community. This normalization was performed to account for significant differences in the richness of the control and *Salmonella*-infected microbial communities, as previously reported (40). FASTA files of the recovered FraBD amino acid sequences are listed in the Data File S1 in the supplemental material. We mined metagenomes from 4 CBA/J mouse metagenomes (NCBI BioProject PRJNA348350).

**qPCR analysis.** We used Jalview (54) to align the FASTA files of all *fraBD* sequences present in the metagenomic DNA libraries of fecal samples from control mice and absent in the highly inflamed *Salmonella*-infected mouse. This alignment, in conjunction with the *Salmonella fraB* sequence, helped identify a 21-nt sequence present in the *fraB* gene of *Clostridium* sp. MGS:81 and notably absent in *Salmonella fraB*. We exploited this distinctive feature and designed a qPCR probe to investigate the change in copy number of *Clostridium* sp. MGS:81 upon *Salmonella* infection, as well as DSS and streptomycin treatment.

Using 5′-AAGAAGGCTAAGGAGAAG-3′ and 5′-GCTGTTGTAATGGATCAG-3′ as the *fraB* forward and reverse primers (Integrated DNA Technologies [IDT], Coralville, IA), respectively, we first obtained a 144-bp PCR amplicon corresponding to the target DNA. This PCR was performed using PrimeSTAR GXL DNA polymerase (Clontech, Mountain View, CA) and control mouse cecum-derived genomic DNA as the template. The 144-bp amplicon was sequenced to ascertain its *bona fides* and validate the specificity of the primers used. Subsequently, a gel-purified preparation of this validated 144-bp amplicon was employed as the standard in our qPCR assays.

All qPCR assays were performed in triplicate using an Applied Biosystems StepOne 48-well instrument and the PerfeCTa qPCR ToughMix (QuantaBio, Beverly, MA) with carboxy-X-rhodamine (ROX) as a passive reference dye. The qPCR probe (IDT) used was 5′-GCGGATGAGTGGTATCAGG-3′ and had a fluor/quencher system consisting of 6-carboxyfluorescein (6-FAM) at the 5′ end, an internal ZEN dark quencher, and an Iowa Black FQ quencher at the 3′ end. Twenty-microliter qPCR mixtures contained 10 ng of cecal contents genomic DNA, 900 nM *fraB* forward and reverse primers, and 250 nM probe (final concentrations). All qPCRs were initiated with a 95°C hold (2 min), followed by 40 cycles of 95°C (3 s), 47°C (15 s), and 68°C (20 s). Three separate runs were conducted to evaluate cecal DNA samples from 25 different mice. Each run contained its own set of negative controls as well as three technical replicates of standard DNA solutions with amounts ranging from 10 pg to 1 fg. The StepOne instrument software determined the threshold normalized fluorescence (ΔRn) values and calculated the $C_T$ values. One threshold ΔRn value was computed for each triplicate set of gDNA samples from each mouse and, likewise, for each set of standards ranging from 1 fg to 10 pg. The threshold values ranged from 0.018 to 0.47 ΔRn units.

## SUPPLEMENTAL MATERIAL

Supplemental material for this article may be found at https://doi.org/10.1128/IAI.00945-17.

**SUPPLEMENTAL FILE 1,** PDF file, 0.2 MB.

**SUPPLEMENTAL FILE 2,** PDF file, 0.1 MB.

## ACKNOWLEDGMENTS

We thank Edward J. Behrman and Alex Bogard for providing fructose-asparagine.

This work was funded by grant number 1R01AI116119 from the National Institutes of Health (to V.G., K.C.W., V.H.W., and B.M.M.A.) and a seed grant from The Ohio State University Foods for Health-Food Innovation Center (to K.C.W., V.H.W., and B.M.M.A.). Part of the research reported here was supported by the NIH National Institute of Allergy and Infectious Diseases (Y1-AI-8401) to J.N.A. and utilized capabilities developed through support from the NIH National Institute of General Medical Sciences (GM094623). Part of the work was performed in the Environmental Molecular Sciences Laboratory, a national scientific user facility located on the campus of Pacific Northwest National Laboratory (PNNL) in Richland, WA, and supported by the U.S. Department of Energy Office of Biological and Environmental Research. Battelle operates PNNL for the DOE under contract no. DE-AC05-76RLO01830.

## REFERENCES

1. Kirk MD, Pires SM, Black RE, Caipo M, Crump JA, Devleesschauwer B, Döpfer D, Fazil A, Fischer-Walker CL, Hald T, Hall AJ, Keddy KH, Lake RJ, Lanata CF, Torgerson PR, Havelaar AH, Angulo FJ. 2015. World Health Organization estimates of the global and regional disease burden of 22 foodborne bacterial, protozoal, and viral diseases, 2010: a data synthesis. PLoS Med 12:e1001921. https://doi.org/10.1371/journal.pmed.1001921.
2. Pires SM, Fischer-Walker CL, Lanata CF, Devleesschauwer B, Hall AJ, Kirk MD, Duarte ASR, Black RE, Angulo FJ. 2015. Aetiology-specific estimates of the global and regional incidence and mortality of diarrhoeal diseases commonly transmitted through food. PLoS One 10:e0142927. https://doi.org/10.1371/journal.pone.0142927.
3. Kotloff KL, Nataro JP, Blackwelder WC, Nasrin D, Farag TH, Panchalingam S, Wu Y, Sow SO, Sur D, Breiman RF, Faruque AS, Zaidi AK, Saha D, Alonso PL, Tamboura B, Sanogo D, Onwuchekwa U, Manna B, Ramamurthy T, Kanungo S, Ochieng JB, Omore R, Oundo JO, Hossain A, Das SK, Ahmed S, Qureshi S, Quadri F, Adegbola RA, Antonio M, Hossain MJ, Akinsola A, Mandomando I, Nhampossa T, Acácio S, Biswas K, O'Reilly CE, Mintz ED, Berkeley LY, Muhsen K, Sommerfelt H, Robins-Browne RM, Levine MM. 2013. Burden and aetiology of diarrhoeal disease in infants and young children in developing countries (the Global Enteric Multicenter Study, GEMS): a prospective, case-control study. Lancet 382:209–222. https://doi.org/10.1016/S0140-6736(13)60844-2.
4. Scallan E, Mahon BE, Hoekstra RM, Griffin PM. 2013. Estimates of illnesses, hospitalizations and deaths caused by major bacterial enteric pathogens in young children in the United States. Pediatr Infect Dis J 32:217–221. https://doi.org/10.1097/INF.0b013e31827ca763.
5. Hoffmann S, Batz MB, Morris JG, Jr. 2012. Annual cost of illness and quality-adjusted life year losses in the United States due to 14 foodborne pathogens. J Food Prot 75:1292–1302. https://doi.org/10.4315/0362-028X.JFP-11-417.
6. Majowicz SE, Musto J, Scallan E, Angulo FJ, Kirk M, O'Brien SJ, Jones TF, Fazil A, Hoekstra RM, International Collaboration on Enteric Disease 'Burden of Illness' Studies. 2010. The global burden of nontyphoidal *Salmonella* gastroenteritis. Clin Infect Dis 50:882–889. https://doi.org/10.1086/650733.
7. Buzby JC, Roberts T. 2009. The economics of enteric infections: human foodborne disease costs. Gastroenterology 136:1851–1862. https://doi.org/10.1053/j.gastro.2009.01.074.
8. Bäumler AJ, Sperandio V. 2016. Interactions between the microbiota and pathogenic bacteria in the gut. Nature 535:85–93. https://doi.org/10.1038/nature18849.
9. Faber F, Tran L, Byndloss MX, Lopez CA, Velazquez EM, Kerrinnes T, Nuccio S-P, Wangdi T, Fiehn O, Tsolis RM, Bäumler AJ. 2016. Host-mediated sugar oxidation promotes post-antibiotic pathogen expansion. Nature 534:697–699. https://doi.org/10.1038/nature18597.
10. Rivera-Chávez F, Bäumler AJ. 2015. The pyromaniac inside you: Salmonella metabolism in the host gut. Annu Rev Microbiol 69:31–48. https://doi.org/10.1146/annurev-micro-091014-104108.
11. Faber F, Bäumler AJ. 2014. The impact of intestinal inflammation on the nutritional environment of the gut microbiota. Immunol Lett 162:48–53. https://doi.org/10.1016/j.imlet.2014.04.014.
12. Nuccio SP, Bäumler AJ. 2014. Comparative analysis of *Salmonella* genomes identifies a metabolic network for escalating growth in the inflamed gut. mBio 5:e00929-14. https://doi.org/10.1128/mBio.00929-14.
13. Lopez CA, Winter SE, Rivera-Chávez F, Xavier MN, Poon V, Nuccio S-P, Tsolis RM, Bäumler AJ. 2012. Phage-mediated acquisition of a type III secreted effector protein boosts growth of *Salmonella* by nitrate respiration. mBio 3:e00143-12. https://doi.org/10.1128/mBio.00143-12.
14. Thiennimitr P, Winter SE, Winter MG, Xavier MN, Tolstikov V, Huseby DL, Sterzenbach T, Tsolis RM, Roth JR, Bäumler AJ. 2011. Intestinal inflammation allows *Salmonella* to use ethanolamine to compete with the microbiota. Proc Natl Acad Sci U S A 108:17480–17485. https://doi.org/10.1073/pnas.1107857108.
15. Winter SE, Thiennimitr P, Winter MG, Butler BP, Huseby DL, Crawford RW, Russell JM, Bevins CL, Adams LG, Tsolis RM, Roth JR, Bäumler AJ. 2010. Gut inflammation provides a respiratory electron acceptor for *Salmonella*. Nature 467:426–429. https://doi.org/10.1038/nature09415.
16. Stecher B, Maier L, Hardt W-D. 2013. "Blooming" in the gut: how dysbiosis might contribute to pathogen evolution. Nat Rev Microbiol 11:277–284. https://doi.org/10.1038/nrmicro2989.
17. Endt K, Stecher B, Chaffron S, Slack E, Tchitchek N, Benecke A, Van Maele L, Sirard J-C, Mueller AJ, Heikenwalder M, Macpherson AJ, Strugnell R, von Mering C, Hardt W-D. 2010. The microbiota mediates pathogen clearance from the gut lumen after non-typhoidal *Salmonella* diarrhea. PLoS Pathog 6:e1001097. https://doi.org/10.1371/journal.ppat.1001097.
18. Stecher B, Robbiani R, Walker AW, Westendorf AM, Barthel M, Kremer M, Chaffron S, Macpherson AJ, Buer J, Parkhill J, Dougan G, von Mering C, Hardt W-D. 2007. *Salmonella enterica* serovar Typhimurium exploits inflammation to compete with the intestinal microbiota. PLoS Biol 5:2177–2189. https://doi.org/10.1371/journal.pbio.0050244.
19. Pilar AVC, Reid-Yu SA, Cooper CA, Mulder DT, Coombes BK. 2012. Active modification of host inflammation by *Salmonella*. Gut Microbes 4:140–145. https://doi.org/10.4161/gmic.23361.
20. Sekirov I, Gill N, Jogova M, Tam N, Robertson M, de Llanos R, Li Y, Finlay BB. 2010. *Salmonella* SPI-1-mediated neutrophil recruitment during enteric colitis is associated with reduction and alteration in intestinal

microbiota. Gut Microbes 1:30–41. https://doi.org/10.4161/gmic.1.1.10950.
21. Ali MM, Newsom DL, Gonzalez JF, Sabag-Daigle A, Stahl C, Steidley B, Dubena J, Dyszel JL, Smith JN, Dieye Y, Arsenescu R, Boyaka PN, Krakowka S, Romeo T, Behrman EJ, White P, Ahmer BMM. 2014. Fructose-asparagine is a primary nutrient during growth of *Salmonella* in the inflamed intestine. PLoS Pathog 10:e1004209. https://doi.org/10.1371/journal.ppat.1004209.
22. Hodge JE. 2002. Dehydrated foods, chemistry of browning reactions in model systems. J Agric Food Chem 1:928–943. https://doi.org/10.1021/jf60015a004.
23. Hansen AL, Behrman EJ. 2016. Synthesis of 6-phosphofructose aspartic acid and some related Amadori compounds. Carbohydr Res 431:1–5. https://doi.org/10.1016/j.carres.2016.05.003.
24. Eichner K, Reutter M, Wittmann R. 1994. Detection of Amadori compounds in heated foods. Thermally generated flavors. ACS Symp Ser 543:42–54. https://doi.org/10.1021/bk-1994-0543.ch005.
25. Anet EFLJ, Reynolds TM. 1957. Chemistry of non-enzymic browning. II. Reactions between amino acids, organic acids, and sugars in freeze-dried apricots and peaches. Aust J Chem 10:182–191.
26. Mossine VV, Mawhinney TP. 2010. 1-Amino-1-deoxy-D-fructose ("fructosamine") and its derivatives. Adv Carbohydr Chem Biochem 64:291–402. https://doi.org/10.1016/S0065-2318(10)64006-1.
27. Maillard LC. 1912. Action des acides aminés sur les sucres. C R Hebd Seances Acad Sci 154:66–68.
28. Sabag-Daigle A, Sengupta A, Blunk HM, Biswas PK, Cron MC, Bogard A, Behrman EJ, Gopalan V, Ahmer BMM. 2017. *Salmonella* FraE, an asparaginase homolog, contributes to fructose-asparagine but not asparagine utilization. J Bacteriol 199:e00330-17. https://doi.org/10.1128/JB.00330-17.
29. Biswas PK, Behrman EJ, Gopalan V. 2017. Characterization of a *Salmonella* sugar kinase essential for the utilization of fructose-asparagine. Biochem Cell Biol 95:304–309. https://doi.org/10.1139/bcb-2016-0138.
30. Sabag-Daigle A, Blunk HM, Sengupta A, Wu J, Bogard AJ, Ali MM, Stahl C, Wysocki VH, Gopalan V, Behrman EJ, Ahmer BMM. 2016. A metabolic intermediate of the fructose-asparagine utilization pathway inhibits growth of a *Salmonella fraB* mutant. Sci Rep 6:28117. https://doi.org/10.1038/srep28117.
31. Sekirov I, Tam NM, Jogova M, Robertson ML, Li Y, Lupp C, Finlay BB. 2008. Antibiotic-induced perturbations of the intestinal microbiota alter host susceptibility to enteric infection. Infect Immun 76:4726–4736. https://doi.org/10.1128/IAI.00319-08.
32. Woo H, Okamoto S, Guiney D, Gunn JS, Fierer J. 2008. A model of *Salmonella* colitis with features of diarrhea in SLC11A1 wild-type mice. PLoS One 3:e1603. https://doi.org/10.1371/journal.pone.0001603.
33. Hapfelmeier S, Hardt W-D. 2005. A mouse model for *S. typhimurium*-induced enterocolitis. Trends Microbiol 13:497–503. https://doi.org/10.1016/j.tim.2005.08.008.
34. Stecher B, Macpherson AJ, Hapfelmeier S, Kremer M, Stallmach T, Hardt WD. 2005. Comparison of *Salmonella enterica* serovar Typhimurium colitis in germfree mice and mice pretreated with streptomycin. Infect Immun 73:3228–3241. https://doi.org/10.1128/IAI.73.6.3228-3241.2005.
35. Faber F, Thiennimitr P, Spiga L, Byndloss MX, Litvak Y, Lawhon S, Andrews-Polymenis HL, Winter SE, Bäumler AJ. 2017. Respiration of microbiota-derived 1,2-propanediol drives *Salmonella* expansion during colitis. PLoS Pathog 13:e1006129. https://doi.org/10.1371/journal.ppat.1006129.
36. Gillis CC, Hughes ER, Spiga L, Winter MG, Zhu W, Furtado de Carvalho T, Chanin RB, Behrendt CL, Hooper LV, Santos RL, Winter SE. 2017. Dysbiosis-associated change in host metabolism generates lactate to support *Salmonella* growth. Cell Host Microbe 23:54–64.e6. https://doi.org/10.1016/j.chom.2017.11.006.
37. Sabag-Daigle A, Wu J, Borton MA, Sengupta A, Gopalan V, Wrighton KC, Wysocki VH, Ahmer BMM. 2017. Identification of bacterial species that can utilize fructose-asparagine. Appl Environ Microbiol 84:e01957-17. https://doi.org/10.1128/AEM.01957-17.
38. Sabag-Daigle A, Blunk HM, Gonzalez JF, Steidley BL, Boyaka PN, Ahmer BMM. 2016. Use of attenuated but metabolically competent *Salmonella* as a probiotic to prevent or treat *Salmonella* infection. Infect Immun 84:2131–2140. https://doi.org/10.1128/IAI.00250-16.
39. Rivera-Chávez F, Winter SE, Lopez CA, Xavier MN, Winter MG, Nuccio S-P, Russell JM, Laughlin RC, Lawhon SD, Sterzenbach T, Bevins CL, Tsolis RM, Harshey R, Adams LG, Bäumler AJ. 2013. *Salmonella* uses energy taxis to benefit from intestinal inflammation. PLoS Pathog 9:e1003267. https://doi.org/10.1371/journal.ppat.1003267.
40. Borton MA, Sabag-Daigle A, Wu J, Solden LM, O'Banion BS, Daly RA, Wolfe RA, Gonzalez JF, Wysocki VH, Ahmer BMM, Wrighton KC. 2017. Chemical and pathogen-induced inflammation disrupt the murine intestinal microbiome. Microbiome 5:47. https://doi.org/10.1186/s40168-017-0264-8.
41. Nuss AM, Beckstette M, Pimenova M, Schmühl C, Opitz W, Pisano F, Heroven AK, Dersch P. 2017. Tissue dual RNA-seq allows fast discovery of infection-specific functions and riboregulators shaping host-pathogen transcriptomes. Proc Natl Acad Sci U S A 114:E791–E800. https://doi.org/10.1073/pnas.1613405114.
42. Mooney JP, Lokken KL, Byndloss MX, George MD, Velazquez EM, Faber F, Butler BP, Walker GT, Ali MM, Potts R, Tiffany C, Ahmer BMM, Luckhart S, Tsolis RM. 2015. Inflammation-associated alterations to the intestinal microbiota reduce colonization resistance against non-typhoidal *Salmonella* during concurrent malaria parasite infection. Sci Rep 5:14603. https://doi.org/10.1038/srep14603.
43. Chassaing B, Srinivasan G, Delgado MA, Young AN, Gewirtz AT, Vijay-Kumar M. 2012. Fecal lipocalin 2, a sensitive and broadly dynamic non-invasive biomarker for intestinal inflammation. PLoS One 7:e44328. https://doi.org/10.1371/journal.pone.0044328.
44. Raffatellu M, George MD, Akiyama Y, Hornsby MJ, Nuccio S-P, Paixão TA, Butler BP, Chu H, Santos RL, Berger T, Mak TW, Tsolis RM, Bevins CL, Solnick JV, Dandekar S, Bäumler AJ. 2009. Lipocalin-2 resistance confers an advantage to *Salmonella enterica* serotype Typhimurium for growth and survival in the inflamed intestine. Cell Host Microbe 5:476–486. https://doi.org/10.1016/j.chom.2009.03.011.
45. Bohnhoff M, Miller CP. 1962. Enhanced susceptibility to *Salmonella* infection in streptomycin-treated mice. J Infect Dis 111:117–127. https://doi.org/10.1093/infdis/111.2.117.
46. Bohnhoff M, Drake BL, Miller CP. 1954. Effect of streptomycin on susceptibility of intestinal tract to experimental *Salmonella* infection. Proc Soc Exp Biol Med 86:132–139. https://doi.org/10.3181/00379727-86-21030.
47. Stevceva L, Pavli P, Buffinton G, Wozniak A, Doe W. 1999. Dextran sodium sulphate-induced colitis activity varies with mouse strain but develops in lipopolysaccharide-unresponsive mice. J Gastroenterol Hepatol 14:54–60. https://doi.org/10.1046/j.1440-1746.1999.01806.x.
48. Mähler M, Bristol IJ, Leiter EH, Workman AE, Birkenmeier EH, Elson CO, Sundberg JP. 1998. Differential susceptibility of inbred mouse strains to dextran sulfate sodium-induced colitis. Am J Physiol 274:G544–G551.
49. Wu J, Sabag-Daigle A, Metz TO, Deatherage Kaiser B, Gopalan V, Behrman EJ, Wysocki VH, Ahmer B. 2018. Measurement of fructose-asparagine concentrations in human and animal foods. J Agric Food Chem 66:212–217. https://doi.org/10.1021/acs.jafc.7b04237.
50. Stojiljkovic I, Bäumler AJ, Heffron F. 1995. Ethanolamine utilization in *Salmonella typhimurium*: nucleotide sequence, protein expression, and mutational analysis of the *cchA cchB eutE eutJ eutG eutH* gene cluster. J Bacteriol 177:1357–1366. https://doi.org/10.1128/jb.177.5.1357-1366.1995.
51. Solden LM, Hoyt DW, Collins WB, Plank JE, Daly RA, Hildebrand E, Beavers TJ, Wolfe R, Nicora CD, Purvine SO, Carstensen M, Lipton MS, Spalinger DE, Firkins JL, Wolfe BA, Wrighton KC. 2017. New roles in hemicellulosic sugar fermentation for the uncultivated Bacteroidetes family BS11. ISME J 11:691–703. https://doi.org/10.1038/ismej.2016.150.
52. Daly RA, Borton MA, Wilkins MJ, Hoyt DW, Kountz DJ, Wolfe RA, Welch SA, Marcus DN, Trexler RV, MacRae JD, Krzycki JA, Cole DR, Mouser PJ, Wrighton KC. 2016. Microbial metabolisms in a 2.5-km-deep ecosystem created by hydraulic fracturing in shales. Nat Microbiol 1:16146. https://doi.org/10.1038/nmicrobiol.2016.146.
53. Altschul SF, Gish W, Miller W, Myers EW, Lipman DJ. 1990. Basic local alignment search tool. J Mol Biol 215:403–410. https://doi.org/10.1016/S0022-2836(05)80360-2.
54. Waterhouse AM, Procter JB, Martin DMA, Clamp M, Barton GJ. 2009. Jalview version 2—a multiple sequence alignment editor and analysis workbench. Bioinformatics 25:1189–1191. https://doi.org/10.1093/bioinformatics/btp033.